Influence of Elevated Pressure on Impingement of a Droplet Upon a Hot Surface

Ilja Buchmüller*, Ilia V. Roisman§, Cameron Tropea§
Institute of Fluid Mechanics and Aerodynamics,
§ Center of Smart Interfaces,
Technische Universität Darmstadt, Germany
buchmueller@sla.tu-darmstadt.de, roisman@sla.tu-darmstadt.de, ctropea@sla.tu-darmstadt.de

Abstract

This study focuses on the qualitative effect of elevated ambient pressure on water droplets with a diameter of 2.4 mm, which accelerate 30 mm, under the influence of gravity, and impact onto a heated surface. A flat aluminum target was heated up to 400 °C (673.15 K) in order to cover nucleate boiling, transition and rebound impact regimes at 1 bar. The experiment is placed in a pressure chamber filled with air at pressures up to 24 bar. This is done to simulate conditions comparable to those of combustion chambers in modern engines. Observations of impact dynamics are made with a high-speed camera at 4000 fps and a high-speed LED stroboscope with flash duration of 300 to 400 ns. The lifetime of a droplet changes according to both the surface temperature and pressure in different boiling regimes. The regime borders shift according to the saturated vapor pressure of the fluid.

Introduction

The conditions of drop impact at high wall temperatures and high ambient pressures are relevant for spray impact onto a wall inside internal combustion engines or in air-blast atomizers for gas turbines. Understanding single drop impact as an element of spray/wall interaction is necessary for describing and modeling spray impact under such conditions.

The ambient pressure has a significant influence on the evaporation rate of an impacting drop because it changes the saturated vapor temperature of the fluid. Therefore, it affects the boiling temperature, the Leidenfrost temperature, the thickness of the vapor layer, and thus the dynamics, the outcome, the heat transfer rates and the parameters of the secondary spray at certain temperatures.

In the present investigation we consider a specialized and simplified case of a single spherical droplet of water descending a short distance in air and impinging onto a hot flat metal target. Evaporation during flight and subsequent condensation during evaporation of the droplet upon the target are neglected. Although simplified, this case is suitable for applications such as high power cooling.

Experimental setup

Comprehensive reviews of the phenomena of drop impact onto an isothermal substrate and of the existing modeling approaches can be found in [1, 2]. These phenomena are mainly governed by drop initial diameter D_0, the impact velocity U_0, surface tension σ, viscosity μ, density ρ and wettability of the solid surface, represented by the equilibrium contact angle θ_e. These parameters can be grouped into the Weber and the Reynolds number given by:

$$We = \frac{\rho D_0 U_0^2}{\sigma};\ Re = \frac{\rho D_0 U_0}{\mu} \tag{1}$$

For a water droplet with the initial size D_0 of approx 2.4 mm and a free fall height of 30 mm, the impact velocity, We and Re are about 0.77 m/s, 19.4 and 1840 respectively. At these parameters, typical for our experiments, the drop does not splash. Numerous studies have been carried out to examine the maximum spread ratio [3, 4]. For a low-viscosity fluid like water the expected maximum spread diameter in this experiment becomes [5]

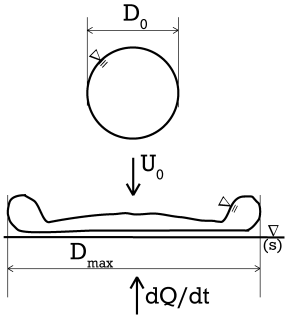

Figure 1. Droplet spread ratio.

$$D_{max} = D_0(0.87Re^{1/5} - 0.4Re^{2/5}We^{-1/2}) \approx 5\ \mathrm{mm} \tag{2}$$

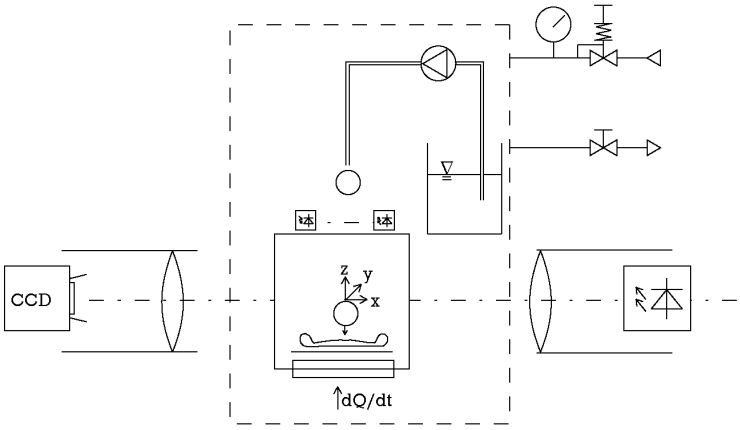

Figure 2. Schematic diagram of the setup.

Similar maximum spread ratios are reported for different fluids [1]. This leads to the size estimation for the heated plate and for the optical access windows. The size of the target plate is chosen to be $25\ \mathrm{mm} \times 25\ \mathrm{mm}$.

The principal design of the setup is shown in figure 2. A piezoelectric pump and a blunt hydrophobic needle are used as a droplet generation device. This simple droplet generation principle was chosen in order to be compact and require only an electrical supply in the pressure chamber during the experiment campaign. Detachment of the individual droplets is induced by pumping under gravitational forces. Measurement and optical systems are synchronized to the detachment of the droplet with a reflective light barrier. The trigger is initiated through an FPGA based measurement system, which incorporates a 100 ms PID temperature controller and protocolling functions. An Ultramic600 heater from Watlow with integrated type K thermocouple is used under the AL99,5 target plate, whose thickness is 3 mm. The target surface is polished with silicone carbide abrasive paper with the grit size P360 and corundum polishing paste to a mirror-like appearance. Electrical insulation of the hot target was enhanced by a ceramic adhesive. Pressure was recorded relative to the ambient pressure of 1018 hPa and 1015 hPa, the pressure sensor has an overall calibrated accuracy of $\pm 0.14\ \%$ of 4 MPa range. The absolute uncertainty in pressure is estimated to be $\pm 60\ \mathrm{hPa} \approx \pm 0.06\ \mathrm{bar}$. A shadowgraphic optic system is implemented, scattering low coherence (coherence length of $4.6\ \mu\mathrm{m}$) blue ($\lambda = 460 \pm 20\ \mathrm{nm}$) light. The stroboscope circuit LDP-V 50-100 V3 with PLCS-21 from PicoLAS, pulsed with the frame rate of the camera (4000 fps) and at a pulse length of 300 ns to 400 ns is used. The light of the LED is collimated with an aspheric lens. The focal length of the camera lens is 300 mm. The pixel size at the object plane is $34.7 \pm 0.2\ \mu\mathrm{m}$ according to calibration pictures.

Considerations on boiling

Evaporation of the droplet can only occur in a phase region where the liquid phase and the gas phase coexist. On the phase diagram shown in figure 3, this is possible on the saturation line, which is also called the boiling curve, found below the critical point and above the triple point of the fluid. At temperatures below the saturation line no boiling phenomena are expected over any time scale.

On the flight to the target the droplet has approximately a spherical shape because of the surface tension and the small capillary length of water. Small amounts of vapor condense on the subcooled droplet and it is heated through radiation from the target; both effects are neglected in the scope of this study. The impact of the droplet on the wall induces bubble entrapment of vapor and ambient gases as well as a hydrodynamic pressure hammer and acoustic waves in and outside the droplet. Because acoustic waves cross a droplet of 2.4 mm diameter at the scale of one microsecond, and the initial impingement process is supposed to have a time scale of 40 ns [6], neither we are yet able to look into that processes nor could we verify any working hypothesis. Therefore we neglect these effects for the present time.

A short contact of two finite bodies with only thermal conduction as a heat transfer mechanism can be modeled using the solution of two semi-infinite bodies [7]. The temperature of the contact point T_m is in this case time-independent and is determined only by the initial temperatures of the droplet and the target, T_d, T_t, and their thermal properties, expressed in the respective thermal effusivities $e = \sqrt{k\, c\rho}$ where k is the thermal conductivity,

*Corresponding author: buchmueller@sla.tu-darmstadt.de

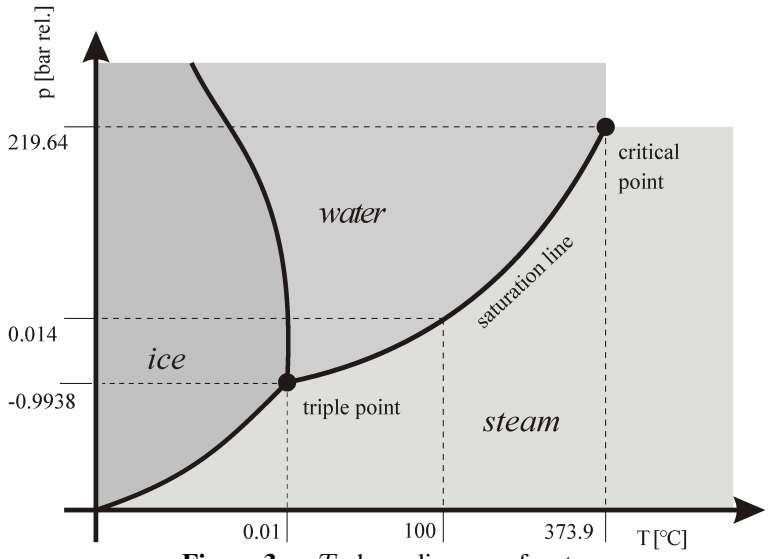

Figure 3. p, T phase diagram of water.

c is the specific heat capacity and ρ is the density:

$$T_m = \frac{e_t T_t + e_d T_d}{e_t + e_d} \tag{3}$$

If the contact temperature is below the saturation temperature the substrate surface will be wetted by the fluid at the first instant and no boiling can be expected. With time the droplet heats up and the contact temperature asymptotically rises to the target temperature, because the droplet is a lot smaller heat sink than the target plate. This may lead to boiling in the long term.

As the contact temperature, which is important for the boiling phenomena, is not accessible directly in our setup, equation (3) is solved for the target temperature. In that way, we can recalculate the short term contact temperature at some phenomenologically interesting measurement point into the corresponding target temperature, which can be controlled and measured easily prior the particular impact.

Vapor can be created at either the existing phase line or a nucleation site. The first process is called evaporation and can be observed in the high-speed photographs. The vapor condenses at some distance from the droplet and the target, generating diffused fog traces. This behavior is shown in figure 4.

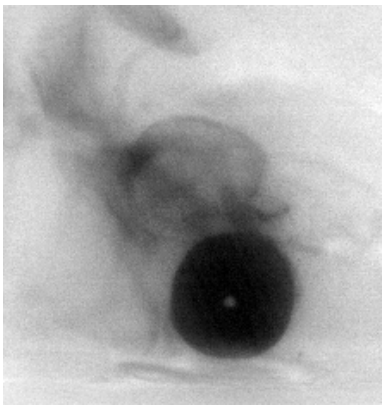

Figure 4. Droplet evaporation before second impact at p=8 bar rel., $T_t = 350$°C.

The second process can be divided into homogeneous and heterogeneous nucleation. For both kinds of nucleation a local overheat of the liquid above the saturation line is necessary [7]. A small vapor bubble of spherical shape at the ambient pressure p a higher pressure p_i inside because of the surface tension at the bubble surface. The pressure difference Δp can be expressed with the Young-Laplace equation:

$$\Delta p = p_i - p = \frac{2\sigma}{R}, \tag{4}$$

where R is the radius of curvature of the interface.

A bubble can be sustained only if the local temperature T is higher than the corresponding saturation temperature by the amount of ΔT, which is derived from the combination of equation (4) with the approximated Clausius-Clapeyron equation for vapor [7, eq. 4.82], using latent heat of evaporation h_{ev}, density of vapor ρ_v and the fluid saturation temperature T_{sat}:

$$\Delta T = T - T_{sat} = \frac{2\sigma T_{sat}}{R \rho_v h_{ev}} \tag{5}$$

In equations (4) and (5) the bubble radius R has to be known or set to a more or less arbitrary value. Otherwise, equation (5) can be solved for R if ΔT is known. The value of the bubble radius is also usually taken as an estimate of a vapor hemisphere above a nucleation site. For homogeneous nucleation this radius is supposed to be quite small, in the range of thermal fluctuations.

Further analysis of heterogeneous nucleation is carried out by the approach shown by Hsu [8], where a thermal boundary layer with a linear temperature drop is considered. The bubble radius is related to the bubble tip distance from the hot wall, the coldest point in the surrounding fluid, which will be touched if the cavity of that particular size is filled with vapor and activated [9]. This model is a good tool for investigations on structured heat exchangers, however, it introduces the thermal boundary layer thickness as a parameter, the measurement of which, inside a moving droplet, is very difficult and probably quite uncertain in accuracy. It should be noted that this layer thickness is reported to be influenced by the fluid motion and the flow velocity at the drop surface. A good overview of the knowledge about heterogeneous nucleation sites and further assumptions are given in [9].

The correlations based on Hsu's criterion generally underestimate the superheat value for the beginning of nucleate boiling [9]. The main reason for this underestimation is the non-occurrence of the cavities in the assumed place when the superheat is sufficient to start boiling.

If the contact temperature is higher, a small disturbance such as the presence of target plate's atoms can trigger the onset of nucleate boiling, despite the target surface being perfectly flat. This leads to boiling of the droplet at any spot of contact with the target, independent of the target's topographic parameters. At higher temperatures all experiments should show non-touching behavior. As this criterion gives the temperature at which the droplet stops touching the surface, here the thermal conduction as a means for heat transfer vanishes. This temperature could be a good candidate for a high lifetime and the beginning of the Leidenfrost regime.

The ability of the vapor to generate a layer that is capable of suspending the droplet in gravity and to cut off thermal conduction could be considered as an alternative criterion for a model. In the approach of Gofftried [10] the Leidenfrost temperature is defined as the lowest temperature with sustainable film boiling. Still, there is an evidence that the variation of the thermal effusivities of the fluid and the target materials leads to the change in the Leidenfrost temperature. That indicates the existence of a (short) conductive fluid/solid contact.

Expected influence of elevated pressure

The main influence of ambient pressure on the heat transfer in the boiling regimes is considered to be the shift in saturation temperature of the vapor. Changes in ambient pressure also lead to slightly different material properties of the fluid; they are usually available in tabulated form for the ranges presented here.

The main difference of the presented setup to already published experiments is that it is possible to switch for different values of the boiling, nucleation and Leidenfrost temperatures in the setup by simply changing the pressure in the experimental chamber.

Results and Discussion

Observations of the phenomena

The measurement points of this investigation have been arranged phenomenologically into different outcome scenarios. The scenarios differentiated were: wetting "I", wetting with boiling "Ib", transition regime "II" and rebound "III". The wetting regime with boiling is a regime of nucleate boiling seen via bubble development; here the droplet acts as a shallow boiling pool. In the transition regime we see periodic detachment of the fluid from the target plate, as some kind of partial dryout. In the third regime droplets rebound without sticking to the target surface, we consider that there is no contact between liquid and solid. These scenarios are depicted in figure 5 with different symbols.

A single droplet, even in wetting regime, is in contact with the wall only at some limited area, depending on the current droplet spread ratio. The area of contact for a droplet with the observed 6.9 mm spread diameter is $A = \pi D^2/4 = 37.3\ \mathrm{mm}^2$. It is assumed that one active nucleate site per droplet is sufficient to initiate nucleate boiling. One site per spread area of $37.3\ \mathrm{mm}^2$ corresponds to the nucleation site density of $N_s = 2.67\ \mathrm{sites/cm}^2$. The empirical superheat value for this site density of bulk water upon a polished aluminium plate ($\theta_e = 30°$) is 8.66 K in this case according to the correlation [9]

$$N_s = 3.4 \times 10^{-5}[1 - cos(\theta_e)]\Delta T^{5.3} \tag{6}$$

An example of the calculations: the contact area dependent nucleation superheat of 8.66°C is added to the saturation temperature of the fluid, 204.32°C for $p = 16$ bar rel. giving a critical value of $T^{\star}_{m,} = 212.98$°C. This

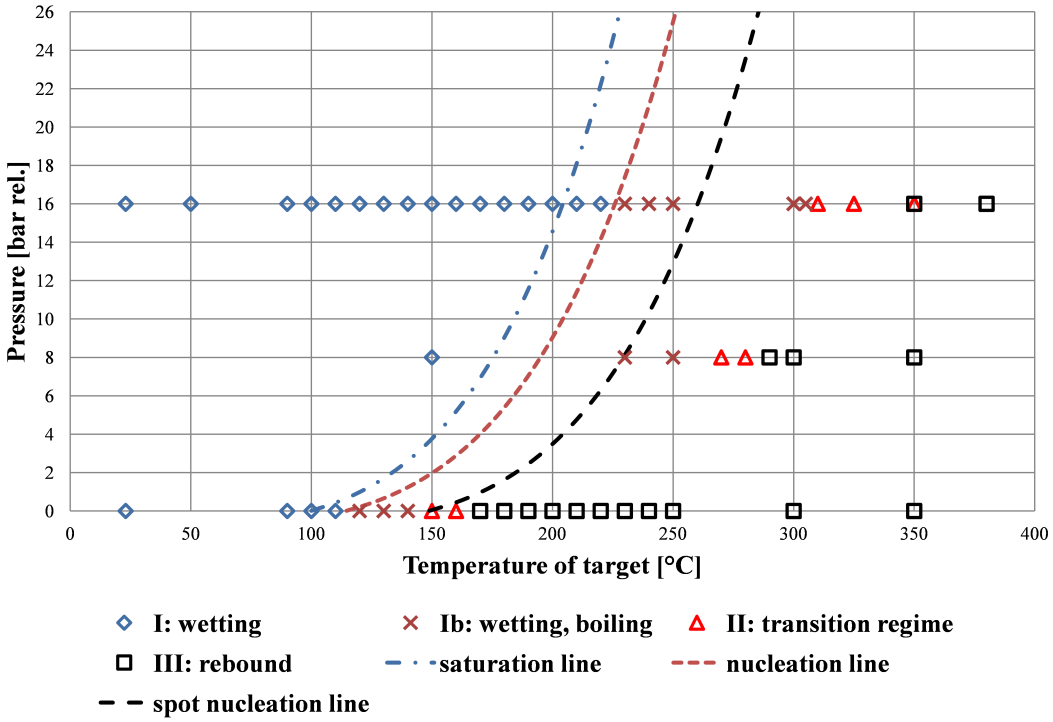

Figure 5. Overview of observed boiling regimes.

value corresponds to the target temperature of $T_t^\star = 225.85$°C according to equation (3). Point P$(T_t^\star, p)$ should mark the regime limit between the impact regimes "I" and "Ib" for the onset of nucleate boiling in the droplet.

In the transition region we have observed droplets partially floating on the vapor layer and periodically touching the wall surface with oscillating parts of the droplet. In such a case the area of contact is a dynamic value and can be quite small. If we assume a contact spot $A = 100\ \mu\text{m} \times 100\ \mu\text{m} = 0.01\ \text{mm}^2$, the corresponding active site density would be $10^4\ \text{sites/cm}^2$. Such a high site density is expected at high wall superheats. However only few experiments with site density over $230\ \text{sites/cm}^2$ and superheat greater than 26 K using water are found in the literature [9]. Using equation (6) we obtain a superheat of 40.89 K estimated for $N_s = 10^4\ \text{sites/cm}^2$ at the border between the nucleate boiling and the transition regime.

The lines in figure 5 show the saturation line from the tabulated values in [11], the nucleation line for the droplet spread diameter of 6.9 mm and the nucleation line for spot areas of $A = 0.01\ \text{mm}^2$, in order to see how theoretical considerations fit with the different outcome regimes. The values for nucleation lines are obtained from the tabulated values in [11] according to the example above.

As can be seen in the figure 5, the plot of the stationary saturation line for bulk liquid is not sufficient to explain the border of the wetting regime "I" and wetted boiling regime "Ib". The nucleation line with superheat for onset of nucleate boiling at the droplet spread area borders the regimes "I" and "Ib". This theory works also at elevated pressure. Therefore we conclude, that the boiling theory with nucleation sites for bulk liquids can also be used in a way that was shown above on a smaller length scale (of 1 mm) for description of droplet impact in the nucleate boiling regime.

The transition regime at $p = 0$ bar rel. extends upto $T_t = 160$°C, i. e. at $T_m = 151.3$°C. The superheat according to equation (6) of 45.9°C corresponds to spot areas of $A = 5.4 \cdot 10^{-3}\ \text{mm}^2 = 5400\ \mu\text{m}^2$. At elevated pressure of $p = 16$ bar rel. the transition regime reaches $T_t = 350$°C, thus $T_m = 329.4$°C. The superheat shifts to 125°C with corresponding spot areas of $A = 2.7 \cdot 10^{-5}\ \text{mm}^2 = 27\ \mu\text{m}^2$ with no apparent explanation. Even with another boiling spot size estimation, present theory would not describe the difference in superheats at the different pressures. A better understanding of pressure effects and fluid dynamics of the oscillating fluid in the transition regime and of the suspended droplet in the rebound regimes is required to explain this anomaly.

The apparent advancing contact angle at the droplet spread ratio of $D = 2$ does not appear to grow with temperature, see figure 6. With rising pressure, the apparent advancing contact angle does also not appear to be influenced. In general the droplets wet the target surface at temperatures below the boiling curve. On the high

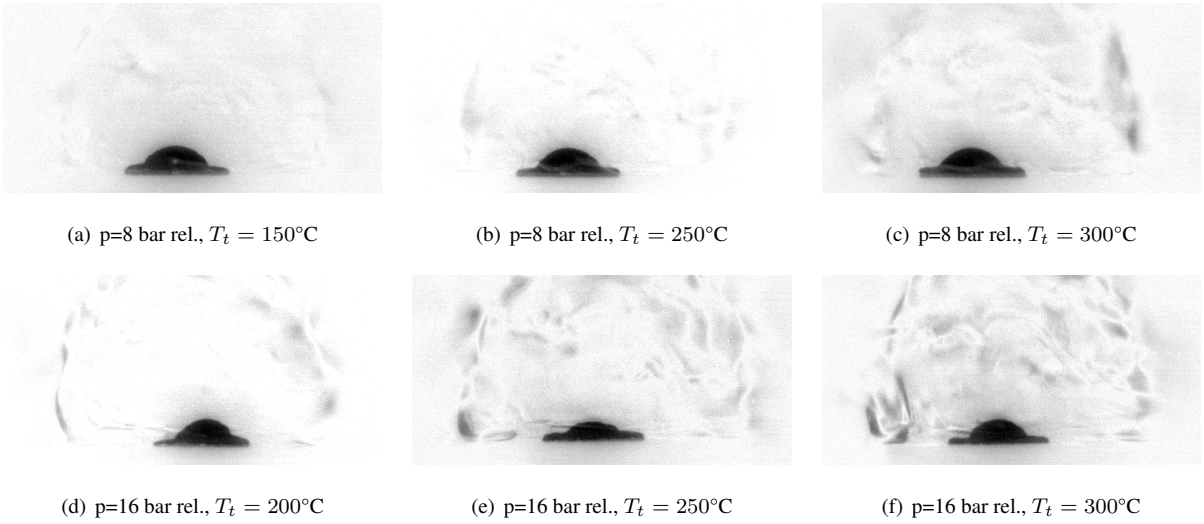

(a) p=8 bar rel., $T_t = 150°C$ (b) p=8 bar rel., $T_t = 250°C$ (c) p=8 bar rel., $T_t = 300°C$

(d) p=16 bar rel., $T_t = 200°C$ (e) p=16 bar rel., $T_t = 250°C$ (f) p=16 bar rel., $T_t = 300°C$

Figure 6. Visualization of droplet impact at different elevated pressures.

temperature side, above Leidenfrost temperature, no wetting is apparent. The behavior in the transition region is still under investigation. Further contact angle measurements are planned.

The lifetime of a droplet is an indirect indicator of the evaporation rate. At temperatures below the vapor saturation temperature the droplet evaporates progressively with rising temperature, the droplet lifetime falls from hours into the range of 10 s. In the boiling regime the evaporation is delayed, due to the contact temperature effect; the evaporation is on a scale of about 5 seconds. When the temperature rises above nucleation superheat, bubbles appear and the lifetime is short, around one second. A minimum lifetime is expected in the nucleate boiling regime, this is also because boiling breaks apart small satellite droplets, as shown in figure 7. At the upper end of the boiling regime the lifetime rises again, despite the rising temperature, because the bubbles merge together. There is a gradual change to the transition regime, the vapor layer starts to appear. Generated vapor is flowing mostly to the sides of the droplet. The maximum in droplet lifetime is another classical definition of the Leidenfrost temperature [12]. With the vapor layer stabilized, heat conduction through contact areas is no longer present, the lifetime can be as high as 120 s. Because radiative and convective heat transport increase with temperature, there is a smooth fall of droplet lifetime in the Leidenfrost regime.

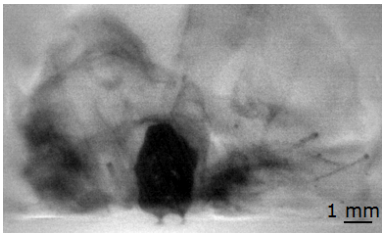

Figure 7. Transition boiling with generation of satellite droplets.

Model of drop evaporation on the substrate

In order to estimate the main factors influencing the phenomena of drop collision with a hot substrate let us consider a one dimensional problem of a droplet on vapor layer with evaporation. Just after impact two thermal boundary layer start to expand in the solid substrate and in the liquid. The solution for these boundary layers is well-known. It leads to the expressions for the heat flux q_d in the droplet at the vapor-liquid interface of the temperature T_{sat} and for the heat flux q_t in the target at its surface in the following form

$$q_d = \frac{e_d(T_{sat} - T_d)}{\sqrt{\pi t}}, \quad q_t = \frac{e_t(T_t - T_m)}{\sqrt{\pi t}}, \tag{7}$$

where T_d and T_t are the initial temperatures of the drop and the target. The contact temperature T_m is not known *a priori* here because of the vapor layer.

The heat flux in the thin vapor layer is estimated through

$$q_v \approx k_v \frac{T_m - T_{sat}}{h(t)}. \tag{8}$$

Combining equations (7) and (8) under assumption of thermal contact at the target surface, $q_t = q_v$, the thickness

of the vapor layer is seen in the form

$$h(t) = A\sqrt{\pi t}\frac{k_v}{e_t}. \tag{9}$$

A is an unknown constant, which will be evaluated from the boundary conditions.

The velocity of vapor at the vapor/liquid interface can be found from the energy balance (Stefan condition) accounting for the continuity of the heat flux at the solid surface, $q_d = q_v$.

$$\frac{dh}{dt} = \frac{q_v - q_d}{\rho_v h_{ev}}, \tag{10}$$

where h_{ev} is the latent heat of evaporation. In this one dimensional model no vapor is assumed to escape radially from the edges of the gap, as this is the case in the central region of the droplet with a thin vapor layer. These conditions yield the following solutions for the contact temperature

$$T_m = \frac{T_{sat} + AT_t}{1 + A}, \tag{11}$$

and the parameter A

$$\frac{Ak_v\sqrt{\pi}}{2e_t} = \frac{(T_t - T_{sat})e_t - (A+1)(T_{sat} - T_d)e_d}{(A+1)h_{ev}\sqrt{\pi}\rho} = 0. \tag{12}$$

An approximate solution of equation (12) for the case of water drop in contact with a high conductivity metal target is

$$A \approx \frac{(T_t - T_{sat})e_t}{(T_{sat} - T_d)e_d} - 1. \tag{13}$$

Therefore the vapor thickness is

$$h(t) = G\sqrt{\pi t}, \quad G = \left[\frac{(T_t - T_{sat})e_t}{(T_{sat} - T_d)e_d} - 1\right]\frac{k_v}{e_t}. \tag{14}$$

The term G is an important parameter of the problem, which determines the rate of drop evaporation on the substrate. G consists only of bulk material properties and measured temperatures and is independent of the pressure in the experiment, giving an opportunity to compare impacts at different pressures. According to equation (14), the vapor thickness increases with time, that corresponds to a movement of the vapor-liquid interface away from the target surface and, on the large scale, to the acceleration of the drop against inertial forces and gravity.

Measurements of the drop life time

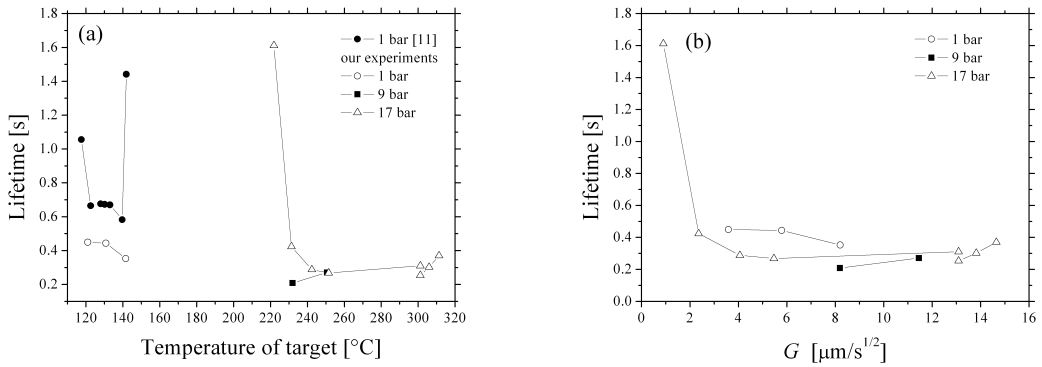

Figure 8. Droplet lifetimes at different pressures as a function of the initial wall temperature (a) and as a function of the parameter G, defined in (14).

Lifetimes of the droplets were measured by counting the frames on the high-speed video. An overview of the lifetimes is given in figure 8. Figure 8a depicts the lifetime data to resolve the measured lifetime minima. In the range below 2 s the lifetimes were measured with the high-speed camera and compared with those of Anokhina [12]. In figure 8b the same data are shown as a function of the parameter G, defined in equation (14). The data, presented in figure 8b lie on approximately one curve, which indicates the relevance of the parameter G to the considered problem. However, it is obvious, that additional data is required to confirm this assumption.

Summary and Conclusions

Four different regimes of droplet evaporation on a hot plate were observed. The limit criteria of these regimes were discussed based on published investigations for boiling of bulk liquids. Even in the setting of single drop impact, the theory, based on nucleation site density in bulk liquids and projected at the contact area of the droplet, explains the measured superheat for onset of nucleate boiling. Taking into account the dependence of the saturated vapor temperature on the surrounding pressure, this theory also explains the measured superheat for onset of nucleate boiling at elevated pressures. However, a similar approach fails to explain the superheats for the transition and rebound regimes. This could be either due to high superheat values, which were not studied in bulk liquids up to now or due to some other phenomenon specific to this experiment, which are yet to be identified.

The apparent advancing contact angle appears to remain constant regardless of the change in temperature and pressure.

The lifetime of droplets under different pressures and temperatures were measured and under ambient pressure proved to be similar to the reported values. A parameter G, obtained from the one-dimensional problem of instationary film boiling, is a term, which helps to model the drop life time at various ambient pressures and wall temperatures.

Acknowledgements

The authors gratefully acknowledge financial support from the Deutsche Forschungsgemeinschaft (DFG) in the framework of SFB-TRR 75 (TP C4).

References

[1] Yarin, A., *Annual Review of Fluid Mechanics* 38:159-192 (2005).
[2] Marengo, M., Antonini, C., Roisman, I. V., and Tropea, C., *Current Opinion in Colloid and Interface Science* 16:292-302 (2011).
[3] Li, R., Ashgriz, N., and Chandra, S., *Journal of Fluids Engineering* 132:061302 (2010).
[4] Roisman, I. V., Rioboo, R., and Tropea, C., *Proceedings of the Royal Society of London. Series A: Mathematical, Physical and Engineering Sciences* 458:1411-1430 (2002).
[5] Roisman, I. V., *Physics of Fluids* 21:052104 (2009).
[6] Engel, O. G., *Journal of Research of the National Bureau of Standards* 54:281-289 (1955).
[7] Baehr, H. D. and Stephan, K., *Wärme- und Stoffübertragung*, Berlin, Heidelberg: Springer, 5th edition, 2006.
[8] Hsu, Y. Y., *Journal of Heat Transfer* 84:207-213 (1962).
[9] Basu, N., Warrier, G. R., and Dhir, V. K., *Journal of Heat Transfer* 124:717-728 (2002).
[10] Gottfried, B., Lee, C., and Bell, K., *International Journal of Heat and Mass Transfer* 9:1167-1188 (1966).
[11] Baehr, H. D. and Kabelac, S., *Thermodynamik: Grundlagen und technische Anwendungen*, Springer, 12th edition, 2005.
[12] Anokhina, E., *Technical Physics* 55:1107-1112 (2010).